ELSEVIER

International Journal of Mass Spectrometry 182/183 (1999) 423–435

International Journal of Mass Spectrometry

Soft landing of ions onto self-assembled hydrocarbon and fluorocarbon monolayer surfaces

Jianwei Shen, Yong H. Yim, Bingbing Feng, Verena Grill, Chris Evans, R. Graham Cooks*

Department of Chemistry, Purdue University, West Lafayette, IN 47907, USA

Received 12 August 1998; accepted 6 October 1998

Abstract

Low energy ($\leq$ 10 eV) ion beams can be soft landed onto a C_{12}-hydrocarbon self-assembled monolayer (H-SAM) surface. The H-SAM surface causes much less collateral fragmentation of the deposited ions under the same conditions than the corresponding fluorinated self-assembled monolayer (F-SAM) surface. The energy dependence for release of ions deposited onto an F-SAM monolayer surface shows that smaller ions are ejected more readily than sterically bulky species. The threshold energy for release of the soft-landed species by $Xe^{+\cdot}$ coincides with that of the typical chemical sputtering product CF_3^+, implying that the deposited species are strongly held inside the SAM matrix and that C–C bond cleavage assists in efficient release of the trapped ions. In cases where fragment ions of the deposited projectile are released from the surface, it is shown, by varying the energy and nature of the releasing projectile ion, that dissociation primarily occurs upon impact of the soft-landed ion and not upon its release. Examination of various odd- and even-electron ions confirms the earlier conclusion that the former are efficiently neutralized and only the latter can be soft landed as ions onto F-SAM surfaces. (Int J Mass Spectrom 182/183 (1999) 423–435) © 1999 Elsevier Science B.V.

Keywords: Soft landing; Ion deposition; Self-assembled monolayers; Energy deposition; Surface-induced dissociation

1. Introduction

Selective chemical modification of surfaces in order to control their physical and chemical properties is a topic of growing interest for its potential applications in technology and material science. Available methods include inter alia, ion implantation [1,2], molecular beam scattering [3,4], chemical vapor deposition [5], and plasma etching [6,7]. Recently we have shown that unique surface modifications can be achieved through soft landing, an experiment in which intact polyatomic ions are deposited at low energy onto an appropriate surface without accompanying dissociation and without neutralization of the ion at the surface [8,9]. The resulting surfaces can be stored for several hours inside or outside the high vacuum chamber with only slow loss of the signals attributed to the deposited ions. The deposited ions can be released intact from the surface by sputtering with low energy ions, often $Xe^{+\cdot}$, or by thermal desorption. The preservation of the intact chemical structure of the deposited ions at a monolayer surface

* Corresponding author.

Dedicated to the memory of Ben S. Freiser, a good friend and stimulating colleague.

PII S1387-3806(98)14251-3

opens potential applications in a number of areas, including studies on the properties and spectroscopy of the isolated ions in monolayer matrices at room temperature. Traditional matrix isolation spectroscopic studies are performed under cryogenic conditions [10]. Moreover, materials containing soft-landed ions have unique properties and hence possible applications in information storage or as molecular "quantum dot" [11,12] structures.

Ion/surface collisions in the low energy regime result (in addition to soft landing) in inelastic scattering, a process described as surface-induced dissociation (SID) [13–16] and in reactive scattering, i.e. ion/surface reactions [17–19]. Much effort has been spent on ion structural characterization [20–22], using inelastic scattering from surfaces. A parallel effort has involved the exploration of ion/surface reactive collisions and the elucidation of their reaction mechanisms and dynamics [23–26]. Soft landing typically occurs at a lower collision energy than that required for either inelastic or reactive scattering, and can itself be accompanied by dissociation and chemical reactions [9]. These latter processes are distinguished from conventional SID and ion/surface reactions by the fact that the products are not scattered from, but are held within, the surface. Evidence for the occurrence of these dissociative and reactive soft-landing processes, in contrast to simple soft landing of intact ions, comes from the release of fragment ions or reaction products from the treated surface [9].

It has been demonstrated that several factors promote successful soft landing. A generalization is that sterically bulky, closed-shell ions that are not fragile to dissociation can be landed intact into fluorinated self-assembled monolayer (F-SAM) surfaces. Examples include various substituted pyridinium cations, methyl or trifluoromethyl-substituted benzoyl ions, disilyl ether cations, and dimethylisothiocyantosilyl ions. Radical cations, such as those of pyridine, benzene, naphthalene, and mono- or ditrifluoromethyl benzonitrile, are not successfully landed at the F-SAM surfaces under the conditions examined so far. Many small even-electron ions, e.g. the dihydrothioisocyantosilyl cation, cannot be efficiently trapped under the same conditions, either. The observation that substituent groups (e.g. methyl or other alkyl groups) facilitate ion deposition suggests that steric constraints and intertwining between the deposited ion and fluoroalkane chains of the surface monolayer play an important role in physically trapping the ions in the interface [9]. The remarkable fact that intact ions, in most cases charge localized even-electron cations, can remain at F-SAM surfaces for long periods, implies that slow neutralization occurs in these highly inert hydrophobic matrices.

In contrast to these room temperature data, Cowin and co-workers have shown that $D_3O^{+\cdot}$ ions can be deposited, as such, into multilayers of *n*-hexane and single crystal D_2O ice films [27]. In addition, Busch and co-workers in contemporaneous work, have demonstrated that metal-containing cluster ions and organic sulfonium ions can be soft landed at metal surfaces [28]. This must be assumed to take place on to the hydrocarbon film known to occur on stainless steel surfaces under ordinary ($\sim 10^{-6}$ Torr) vacuum conditions. The results from these groups suggest that polyatomic ions might be soft landed onto hydrocarbon self-assembled monolayer (H-SAM) surfaces, an experiment that logically extends our earlier F-SAM studies [8,9].

In this article we demonstrate surface modification through soft landing of ions onto an H-SAM surface. We compare soft landing onto F-SAM and H-SAM surfaces. We also examine the fragmentations and ion/surface reactions that can accompany soft landing by varying the energies at which the landing and the diagnostic ion release experiments are performed. It has long been known that hydrocarbon self-assembled monolayer surfaces are "softer" than fluorocarbon surfaces in inelastic ion/surface collisions, viz. they display relatively lower translational to internal energy conversion [29–31]. This can be considered a disadvantage in the use of H-SAM surfaces for activating large biological and other refractory ions for structural characterization by SID. However, the relative softness of the H-SAM surface might be beneficial to the preservation of the intact molecular ion structure in soft-landing experiments. There is also much regarding the energetics of the soft-landing process and the mechanism of trapping at the interface

that is not yet known. Comparative studies of soft landing onto various surfaces should help provide understanding of these issues.

2. Experimental

Experiments were performed using a custom-built hybrid mass spectrometer of BEEQ (B = magnetic sector, E = electrostatic analyzer, Q = quadrupole mass analyzer) configuration [32]. Projectile ions were generated by 70 eV electron ionization (EI) and were mass selected and energy focused using the B and first E analyzers. Prior to collision, the 2 keV ion beam was decelerated to the desired translational energy with respect to the F-SAM target surface, which was held in a UHV chamber at a nominal pressure of 2–5 $\times$ 10^{-9} Torr. The nominal laboratory collision energy was calculated as the difference in potential between the ion source and target. The measured potentials typically have a $\pm$ 2 eV uncertainty below 20 eV, and $\pm$ 1 eV above. For most surface analysis and ion/surface collision studies, the ion beam was inclined at 55° with respect to the surface normal, whereas the lens system used for extraction of scattered secondary ions was held at 90° with respect to the incoming beam. Scattered product ions were extracted into the post-collision E and Q analyzer system and were mass analyzed using the quadrupole mass analyzer. Data are recorded in thomson, where 1 thomson (Th) = 1 Dalton per unit charge [33]. For the surface modification experiments, the angle of incidence with respect to the surface normal was set to 0° to maximize the efficiency of ion deposition. The surface current was monitored using a Keithley model 485 picoammeter that was floated at the target potential.

Gas-phase collision-induced dissociation was performed using a custom-built pentaquadrupole mass spectrometer [34]. The ions of interest were generated by 70 eV EI, mass selected using Q1 and dissociated in Q4 by collision with argon at 10 eV (the potential difference between the collision quadrupole and the ion source). The collision cell pressure was increased from 3 $\times$ 10^{-5} to 6 $\times$ 10^{-5} Torr upon addition of argon gas to Q4. The resulting product ions were analyzed by scanning Q5.

N,*N*-Dimethyl-*p*-toluidine, carbon disulfide, and methyl iodide were purchased from Aldrich (Milwaukee, WI), and high purity xenon was obtained from Airco (Murry Hill, NJ). The F-SAM and H-SAM surfaces were made and cleaned in house, following literature procedures [35]. 1,2-Tetrahydroperfluorodecane disulfide ($(CF_3(CF_2)_7\text{-}(CH_2)_2S)_2$) and 1-mercaptododecane ($CH_3(CH_2)_{11}SH$) were used to form the self-assembled monolayer surfaces by exposure of the gold surface to their ethanolic solutions for two weeks. The fresh surfaces were rinsed with anhydrous ethanol and dried with nitrogen gas before introduction into the UHV chamber.

3. Results and discussion

3.1. Soft landing of the N,N-dimethyl-p-toluidine $(M\text{-}1)^+$ ion onto a C_{12} H-SAM surface

Fig. 1(a) shows the mass spectrum of a freshly prepared H-SAM surface subjected to 65 eV xenon ion bombardment. Almost all the peaks are attributed to ions characteristic of chemical sputtering (i.e. charge exchange with release of the ionized material previously bound to the surface [36]) and are typical of hydrocarbon surfaces examined in this way. These ions include $C_2H_3^+$ (*m*/*z* 27), $C_2H_5^+$ (*m*/*z* 29), $C_3H_3^+$ (*m*/*z* 39), $C_3H_5^+$ (*m*/*z* 41), $C_3H_7^+$ (*m*/*z* 43), $C_4H_7^+$ (*m*/*z* 55), and $C_4H_9^+$ (*m*/*z* 57). Also observed are two peaks, *m*/*z* 83 and *m*/*z* 100, that are believed to originate from adventitious hydrocarbon contaminates. It is worth noting that prior to soft landing, *m*/*z* 134, 119, 118, and 91 are essentially absent. Onto this surface were deposited $(M\text{-}1)^+$ ions (*m*/*z* 134) derived from *N*,*N*-dimethyl-*p*-toluidine. Soft landing was performed at a collision energy of 8 $\pm$ 2 eV for 1 h using an indicated ion current of 0.5 $\times$ 10^{-9} A and a spot size estimated as 50 mm^2. In order to maximize the deposition efficiency, the incident angle of the ion beam was set to 0° with respect to surface normal, and the post-collision extraction lens voltage was raised to that of the surface. After ion deposition,

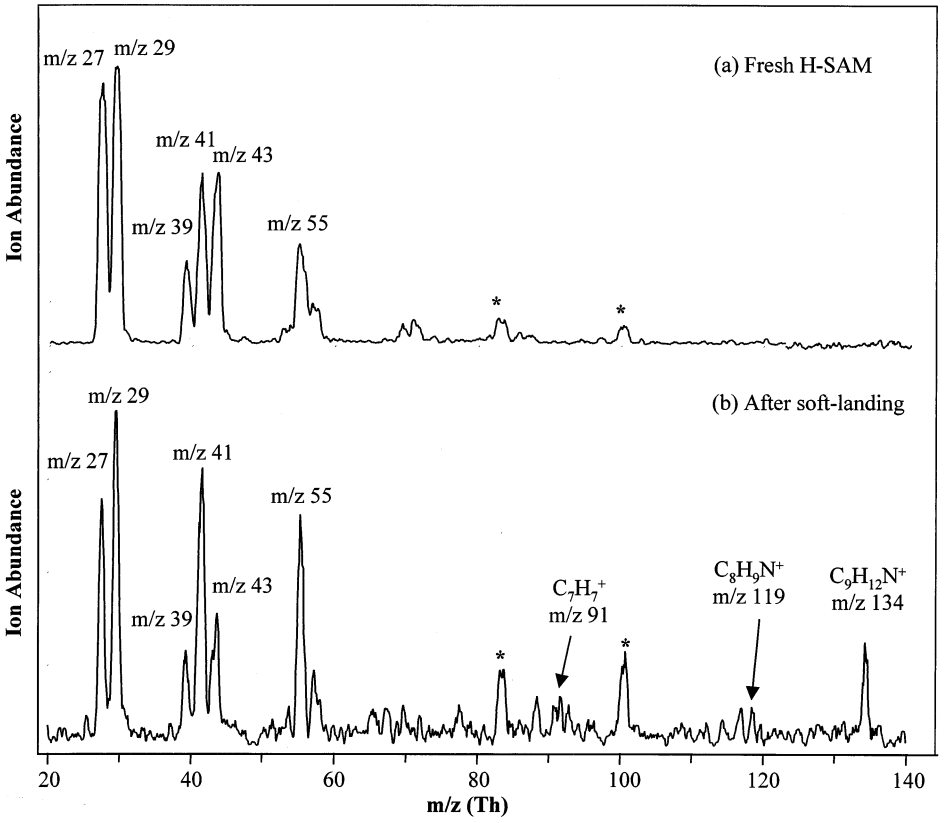

Fig. 1. Sputtering spectra of an H-SAM surface (65 eV $Xe^{+\cdot}$) (a) before, and (b) after surface modification through soft landing of *N*,*N*-dimethyl-*p*-toluidine $(M\text{-}1)^+$ (*m*/*z* 134) at a collision energy of 8 ± 2 eV for 1 h (nominal beam current, 0.5×10^{-9} A).

the surface was subjected to 65 eV $^{129}Xe^{+\cdot}$ sputtering analysis [Fig. 1(b)]. The major new feature of the spectrum is a peak at *m*/*z* 134. Although the noise level is relatively high, additional minor peaks at *m*/*z* 119, 118, and 91 are also noticeable. The relative abundance of the *m*/*z* 134 ion is about 25% of the base peak, *m*/*z* 29, in the full mass spectrum. The observation of the feature at *m*/*z* 134 clearly establishes that the projectile ion is successfully deposited, intact, on the H-SAM surface.

Gas-phase collision-induced dissociation (CID) experiments indicate that the $(M\text{-}1)^+$ ion of *N*,*N*-dimethyl-*p*-toluidine fragments to *m*/*z* 91 ($C_7H_7^+$), 118 ($C_8H_8N^{+\cdot}$), and 119 ($C_8H_9N^+$) upon multiple argon collisions (Fig. 2). The CID result clearly shows that the chosen $(M\text{-}1)^+$ (*m*/*z* 134) ion is relatively stable, and also that its fragmentation products are identical in the gas and surface collision experiments. Thermochemical data on the chosen $(M\text{-}1)^+$ ion (*m*/*z* 134) are not available, although the bond dissociation energy for the aromatic C–N bond is estimated to be 3.8 eV from the following reaction for a related model system for which the necessary thermochemical information is available in the literature [37,38]:

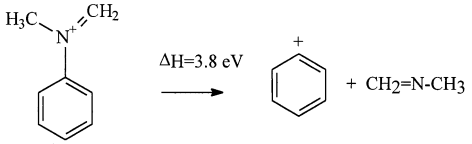

Scheme 1.

For H-SAM surfaces, about 13% of the initial translational energy is converted into vibrational en-

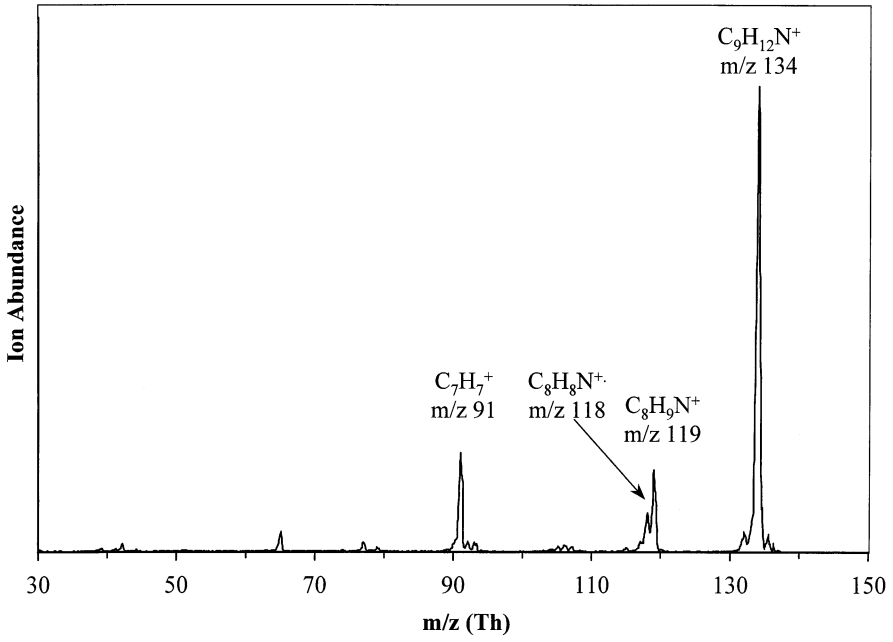

Fig. 2. CID product ion spectrum showing fragmentation of *N*,*N*-dimethyl-*p*-toluidine $(M\text{-}1)^+$ (*m*/*z* 134) at collision energy of 10 eV.

ergy of the projectile ion in the course of inelastic collisions [39]. Note that the above energy conversion factor applies to ions that are inelastically scattered in a single collision event. In the course of soft landing, ions will penetrate into the matrix and experience multiple collisions. Therefore, a much higher fraction of their energy can be expected to be converted into internal energy of the projectile. Nevertheless, assuming that the 13% $T \rightarrow V$ conversion value sets the lower limit for the ion internal energy in the soft-landing experiment, the minimum energy deposited is about 1 eV at a collision energy of 8 eV. The xenon sputtering data [Fig. 1(b)] indicates that a certain amount of dissociation accompanies 8 eV soft landing on the H-SAM, as represented by the fragment ions observed at *m*/*z* 91, 118, and 119. From the estimated bond energy of 3.8 eV, this result suggests that the $T \rightarrow V$ conversion factor in soft landing is much greater than the factor for single inelastic collisions, although the amount cannot be more accurately quantified. Note also that impulsive energy transfer to the surface is the other main energy sink. In the course of inelastic scattering it is known that $> 70\%$ of the translational energy is deposited in this way [29]. This energy could strongly disturb the SAM chains and create a disordered region in which the projectile ions might be trapped.

In the course of examining the modified surface by xenon sputtering, it is possible that some of the $Xe^{+\cdot}$ collision energy is transferred to the deposited ions by momentum transfer. These ions might then leave the surface internally excited, and this is an alternative explanation for the fragmentation pattern seen in the release ($Xe^{+\cdot}$) spectrum. To investigate this possibility the xenon collision energy was varied. Table 1

Table 1
Relative abundance of the deposited species as a function of $Xe^{+\cdot}$ sputtering energy after the H-SAM modified by 10 eV soft landing of *N*,*N*,-dimethyl-*p*-toluidine $(M\text{-}1)^+$ ion (*m*/*z* 134)

Collision energy (eV)	Relative abundance			
	m/*z* 134	*m*/*z* 119	*m*/*z* 118	*m*/*z* 91
50	100	20	28	34
65	100	27	28	17
85	100	33	33	35
105	100	33	33	32

Table 2
Sputtering analysis using 65 eV CF_3^+, I^+, and $Xe^{+\cdot}$ ion impact on an H-SAM modified by soft landing of *N*,*N*-dimethyl-*p*-toluidine $(M\text{-}1)^+$ ion (*m*/*z* 134)

Projectile ion	Recombination energy (eV)	Abundance ratio [*m*/*z* 134]/ Σ[deposited ion][a]	Relative sputtering yield (%)[b]
CF_3^+ (*m*/*z* 69)	9.3	0.47	0.31
I^+ (*m*/*z* 127)	10.2	0.52	1.16
$Xe^{+\cdot}$ (*m*/*z* 129)	12.13	0.58	1.00

[a] Σ[deposited ion] includes ion abundance of *m*/*z* 134, 119, 118, and 91.

[b] Sputtering yield is defined as: Σ[deposited ions]/beam current. The deposited ions include ions *m*/*z* 134, 119, 118, and 91. The calculated value was normalized with respect to the result of $^{129}Xe^{+\cdot}$ sputtering to give the relative yield.

summarizes the relative abundance of the ions observed after 10 eV soft landing as a function of xenon ion energy. In all cases the deposited species *m*/*z* 134 appears as the major ion. Interestingly, even though the xenon collision energy is varied from ~ 50–100 eV, the relative abundance of the fragment ions does not increase a great deal. This suggests that xenon inelastic collisions largely release the "preformed" deposited ions. In other words, fragmentation of the deposited species occurs mainly during the landing rather than in the release process. Similar results are obtained for F-SAM surfaces as discussed below.

Our previous data [8,9] on soft landing of ions onto F-SAM surfaces suggest that physical sputtering (momentum transfer through binary elastic collisions) is responsible for the release of the deposited ions from the matrix. Chemical sputtering with associated charge exchange of the trapped species is not involved; however, charge exchange with the fluorocarbon chains appears to facilitate release of the deposited ion [9]. Table 2 summarizes the results of experiments on characterization of the modified H-SAM surface using different projectile ions. It is important to note that the ratio of the deposited ion *m*/*z* 134 to all the fragments of the deposited species changes by only a small amount and the ion *m*/*z* 134 is the most abundant species in all three sputtering experiments. In contrast to the cases of I^+ and $Xe^{+\cdot}$ as projectiles, which give similar sputtering yields, the yield is much lower when using the lighter CF_3^+ ion. However, there appears to be no correlation between the recombination energy (RE) of the projectile and its releasing efficiency. If the ejected ions are formed only by charge exchange between the projectile ion and a neutralized deposited species, the CF_3^+ ion (IE = 9.3 eV), presumably closer in IE to the deposited species, should give most efficient sputtering. The results suggest that the heavy ions $Xe^{+\cdot}$ or I^+ are more efficient in releasing the deposited species. This null hypothesis argument, which is consistent with previous F-SAM data, again implies that physical (momentum transfer) sputtering rather than charge exchange is dominant in the ejection of the deposited species and that these are indeed present as ions within the H-SAM matrix. The data are also consistent with the notion that C–C bond cleavage by charge exchange facilitates release. This is suggested by the fact that the signal is a maximum for I^+ which has an RE that matches the IE of the surface.

The above results clearly demonstrate that polyatomic ions can be deposited intact, i.e. soft landed, onto hydrocarbon surfaces. It is reasonable to assume that the ion trapping mechanism in the H-SAM case is similar to that which operates for F-SAM surfaces, even though adventitious hydrocarbon adsorbates (which could build up in the course of deposition) could complicate the trapping mechanism. The common features between the H-SAM and F-SAM experiments include the fact that both H-SAM and F-SAM surfaces are highly hydrophobic and chemically inert, which is expected to minimize reaction between the trapped ions and traces of gaseous reactive species. In both cases, the chosen ion is especially favorable for soft landing; in particular, the methyl groups on the aromatic ring and on the nitrogen atom probably provide the necessary steric constraint to physically hold the species in the monolayer. The probable low RE of the deposited $(M\text{-}1)^+$ ion (for the radical cation of *N*,*N*-dimethyl-*p*-toluidine, RE = 6.93 eV) and high ionization energy for the matrix (estimated using *n*-C_8H_{18}, IE = 9.80 eV [38]) presumably contribute to a low rate of the neutralization. It has been estimated that as much as 2 eV or more electrostatic binding by image potentials could occur for ions trapped near metal surfaces [9].

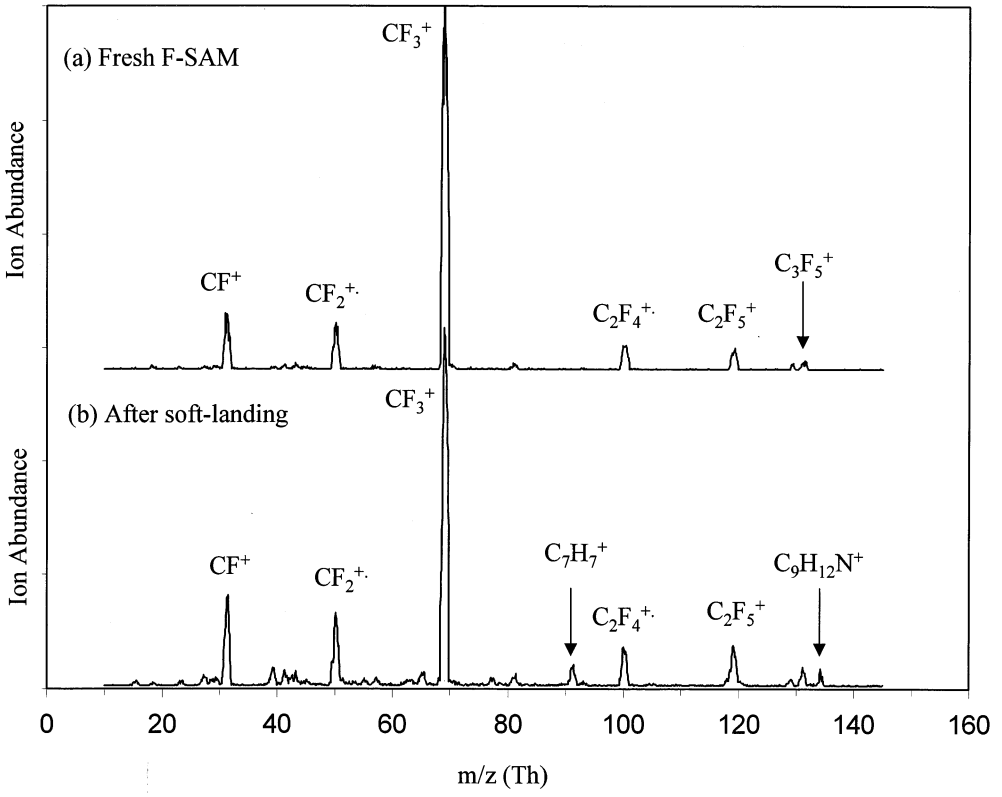

Fig. 3. Sputtering spectra of an F-SAM surface (65 eV $Xe^{+\cdot}$) (a) before, and (b) after surface modification through soft landing of *N*,*N*-dimethyl-*p*-toluidine $(M\text{-}1)^+$ (*m*/*z* 134) at a collision energy of 7 ± 2 eV for 1 h.

3.2. Soft landing of the N,N-dimethyl-p-toluidine (M-1)$^+$ ion onto a C10 F-SAM surface

It has long been known that an F-SAM surface is a "harder" target for affecting projectile ion activation than is an H-SAM surface. Conversion efficiencies of 20–30% (*T*-to-*V*) have been reported for inelastic scattering [39,15]. It is of interest to examine the surface effects on soft landing in a parallel experiment, by comparing soft landing of *N*,*N*-dimethyl-*p*-toluidine $(M\text{-}1)^+$ (*m*/*z* 134) on an F-SAM surface with the corresponding H-SAM results.

As before, $^{129}Xe^{+\cdot}$ sputtering at a collision energy of 65 eV was used to establish the behavior of the virgin surface. Fig. 3(a) shows only typical chemical sputtering products, e.g. CF^+, $CF_2^{+\cdot}$, CF_3^+, $C_2F_4^{+\cdot}$, $C_2F_5^+$. However, after deposition of the ion of *m*/*z* 134 for 1 h at a collision energy of 7 ± 2 eV, subsequent $Xe^{+\cdot}$ sputtering at 65 eV revealed a distinct peak at *m*/*z* 134. This clearly indicates that the chosen ion (*m*/*z* 134) was successfully deposited at the surface [Fig. 3(b)]. Also important is that an almost equally abundant ion is observed at *m*/*z* 91, as is a trace *m*/*z* 118 peak, poorly resolved from *m*/*z* 119. In contrast to the results on the H-SAM surface, the appearance of these ions indicates that extensive dissociation occurs during ion landing onto the F-SAM surface.

The ejection of the deposited $(M\text{-}1)^+$ ion from the F-SAM surface by $Xe^{+\cdot}$ sputtering shows a strong dependence on collision energy. This is illustrated in Fig. 4. As the $Xe^{+\cdot}$ collision energy was varied from 30–100 eV, the relative abundances of *m*/*z* 91 and 134 change considerably. At 30 eV collision energy, only the *m*/*z* 91 ion was detected whereas the *m*/*z* 134 ion was almost absent. As the collision energy

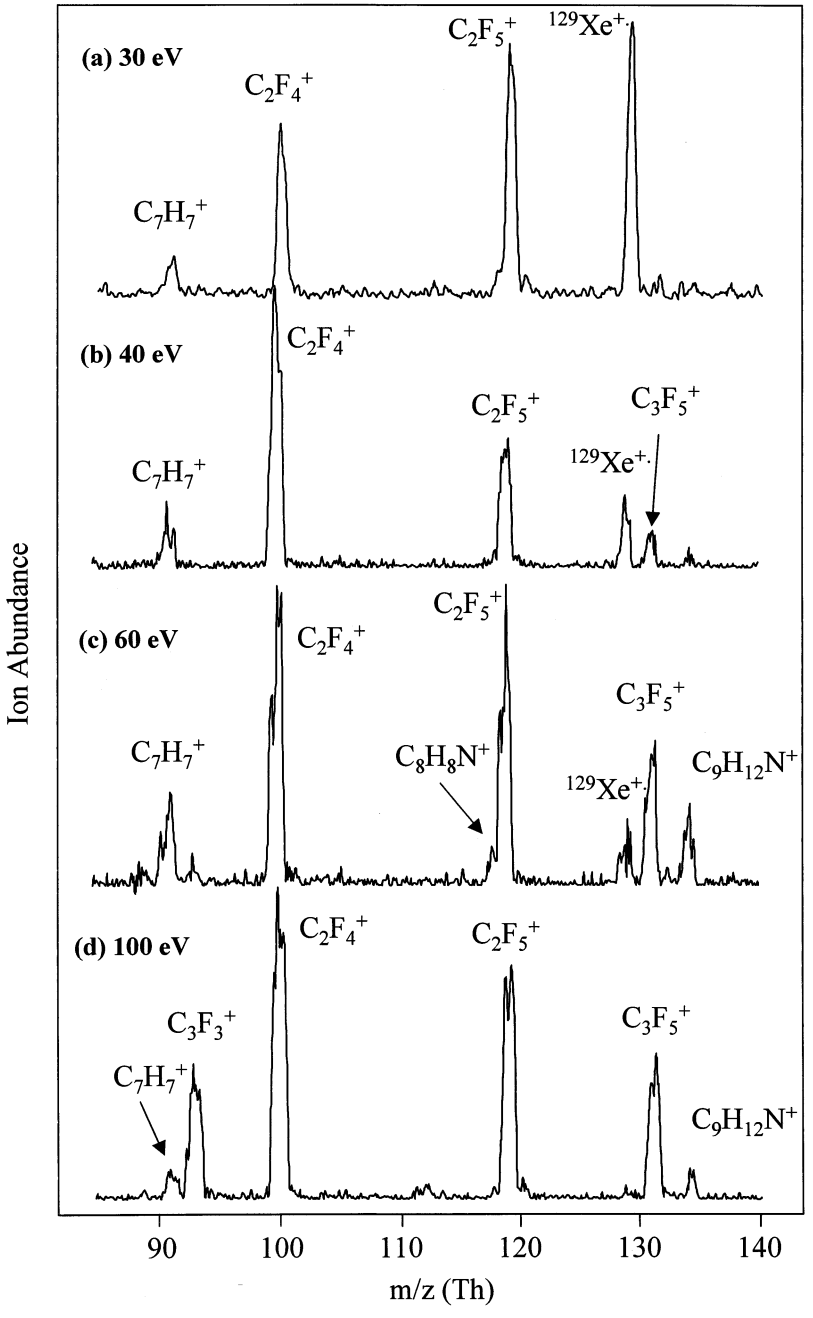

Fig. 4. Mass spectra recorded upon the collision of $Xe^{+\cdot}$ at various collision energies on an F-SAM surface after soft landing of *m*/*z* 134 ion.

was raised to 60 eV, almost equal abundances of *m*/*z* 91 and 134 were observed. A further increase in energy collision to 100 eV seems not to affect the ratio of *m*/*z* 91 and 134. This behavior should be contrasted with that already reported in Table 1 for deposition onto the H-SAM surface. The large fragment ion abundance observed at the F-SAM even at low collision energy suggests that the energy imparted

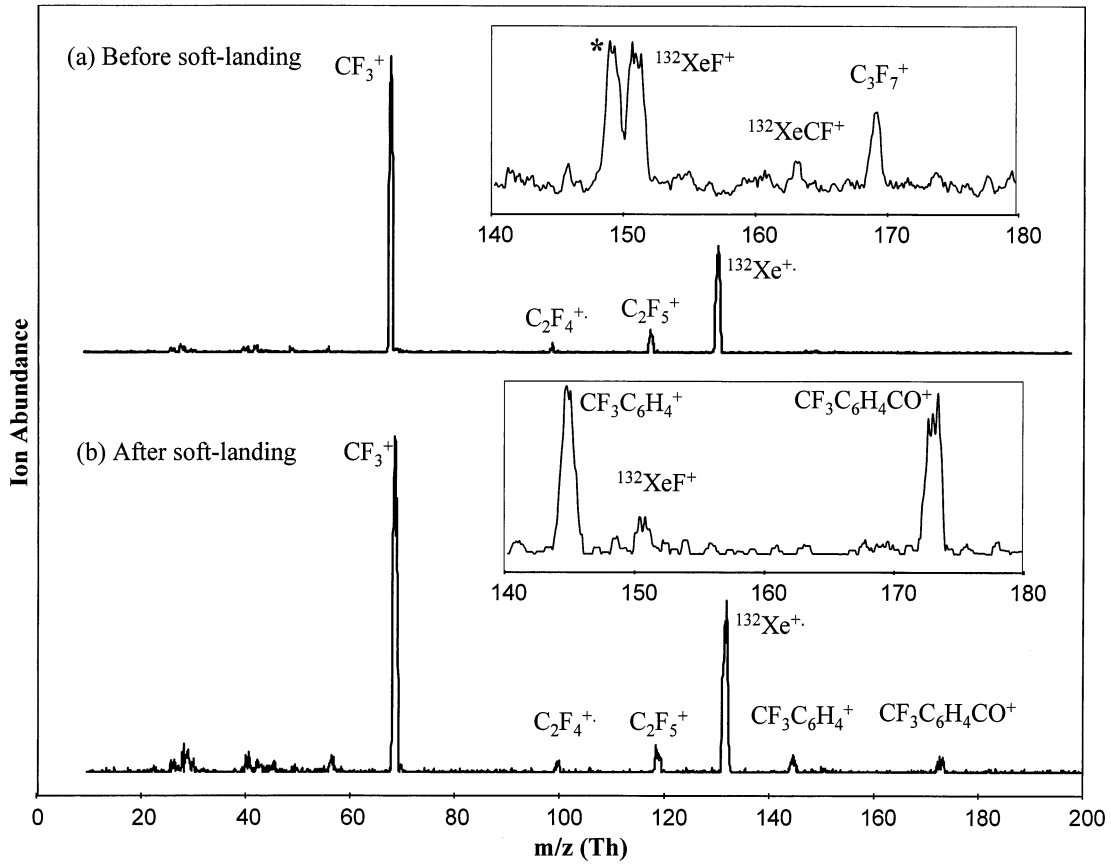

Fig. 5. Mass spectra upon the collision of $Xe^{+\cdot}$ at 30 eV from the surface (a) before, and (b) after soft-landing modification with *m*-trifluoromethylbenzoyl ion (*m*/*z* 173) at a collision energy of ~ 10 eV for 5 h. The peak at *m*/*z* 149 (labeled with an asterisk) is a phthalate contaminant at the surface.

by $Xe^{+\cdot}$ collisions is not responsible for the observation of fragment ions. This conclusion is in agreement with that reached earlier. However, the data also demand the conclusion that the ejection efficiency for the soft-landed fragment ions varies uniquely with the sputtering energy. The latter conclusion is understandable since the deposited ions are presumably sterically trapped and stabilized within the long alkyl chain matrix from which the smaller fragment ions are more readily released. The data appear to be consistent with the previous proposed "intertwining" trapping mechanism [8]. Independent experiments in which soft landing of smaller ions such as $C_7H_7^+$ and $C_6H_5^+$ were attempted all showed negligible landing results, implying that the binding force for sterically less hindered ions such as $C_7H_7^+$ (*m*/*z* 91) in the F-SAM matrix is far weaker.

3.3. Soft-landing of m-trifluoromethylbenzoyl ion onto a C_{10} F-SAM surface

In the course of exploring the effect of the even/odd electron nature of the projectile cation on the soft-landing efficiency, *m*-trifluoromethylbenzoyl cation (*m*/*z* 173), generated from 70 eV EI of 3-(trifluoromethyl)benzophenone, and the radical cation 3-(trifluoromethyl)benzonitrile (*m*/*z* 171), were examined. Both of these ions, presumably, should have similar structures except for the inclusion of the heteroatom substitution and their contrasting odd/

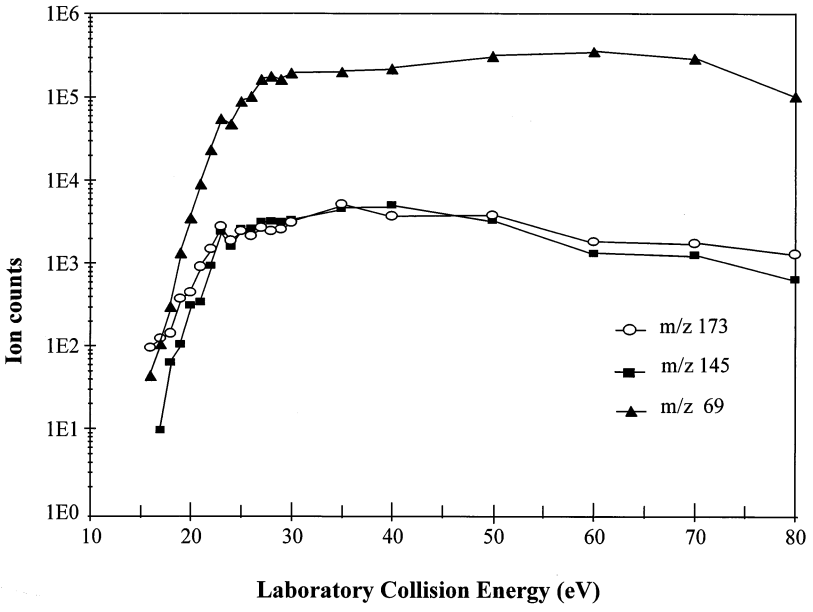

Fig. 6. Dependence of the deposited ion and sputtering product yield on the $Xe^{+\cdot}$ collision energy used to sample an F-SAM surface modified by soft landing of ion *m*/*z* 173.

even electron natures. Fig. 5 displays the 30 eV $^{132}Xe^{+\cdot}$ sputtering spectra before and after surface modification through ~ 10 eV deposition of the benzoyl ion, *m*/*z* 173, for 5 h. Collisions of 30 eV $Xe^{+\cdot}$ with a fresh F-SAM [Fig. 5(a) and insert] lead to typical chemical sputtering products e.g. CF_3^+ (*m*/*z* 69), $C_2F_4^{+\cdot}$ (*m*/*z* 100) and $C_3F_7^+$ (*m*/*z* 169), along with various ion/surface reaction products, including XeF^+ (*m*/*z* 151) and $XeCF^+$ (*m*/*z* 163) discussed previously [24]. After soft-landing of *m*/*z* 173, 30 eV $^{132}Xe^{+\cdot}$ sputtering showed additional peaks at *m*/*z* 173 and 145 [Fig. 5(b)]. The latter corresponds to the loss of the carbonyl group of the deposited benzoyl cation (*m*/*z* 173). Note that even after 5-h deposition with an estimated total dose of 5×10^{13} ions in an area of 50 mm^2, the abundances of *m*/*z* 173 and 145 remain relatively small. This result suggests that the overall efficiency of soft landing or of its detection is low.

In contrast to the behavior of *m*-(trifluoromethyl) benzoyl cation, after soft landing of 3-(trifluoromethyl)benzonitrile molecular ion, under similar conditions, subsequent $Xe^{+\cdot}$ sputtering in the collision energy range of 30–80 eV did not produce *m*/*z* 171 ion or any corresponding fragment ions. Other radical cations with similar structures, including methyl-, dimethyl-, and the bis(trifluoromethyl)-substituted benzonitriles also failed to be trapped in the F-SAM matrices. On the other hand, bis(trifluoromethyl)benzoyl cation gives similar results to the mono-substituted benzoyl cation and shows analogous peaks at *m*/*z* 241 and 213 upon subsequent $Xe^{+\cdot}$ sputtering. The striking difference between the even-electron cations and radical cations indicates that the availability of an unfilled orbital promotes electron transfer and precludes soft landing of the ion in its charged form.

The energy dependence of $Xe^{+\cdot}$ sputtering after *m*-(trifluoromethyl)benzoyl ion deposition is displayed in Fig. 6. Also shown is the abundance of CF_3^+—the characteristic product of chemical sputtering of F-SAM surfaces. Note that the appearance energy (~ 18 eV) of the deposited species (*m*/*z* 173 and 145) almost coincides with that of CF_3^+. Also note the nearly equal abundance of *m*/*z* 173 and 145 observed throughout the entire collision energy range

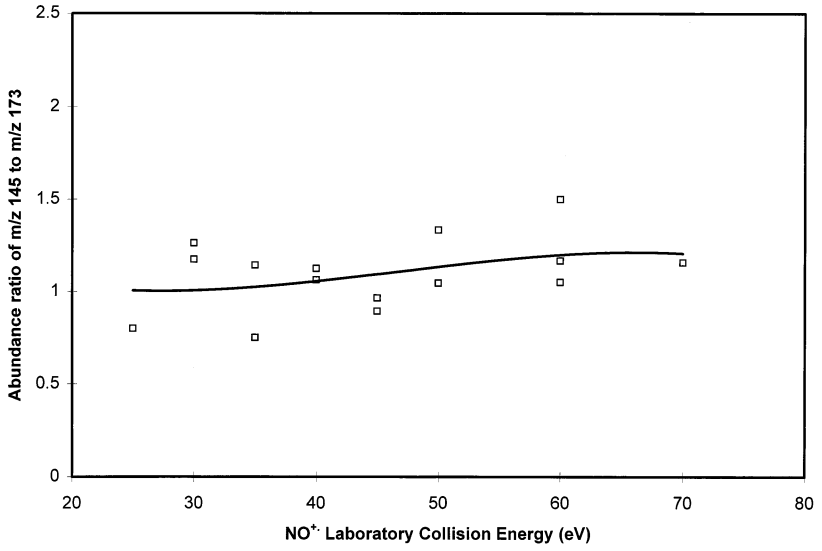

Fig. 7. Dependence of the deposited ion and fragmentation product yield on the $NO^{+\cdot}$ collision energy used to sample an F-SAM surface modified by soft landing of ion m/z 173.

from 15–80 eV. The first point is reminiscent of earlier results on soft landing of $(CH_3)_2SiNCO^+$ (m/z 116) that is released at an appearance energy similar to that of $C_2F_5^+$ [9]. This observation again suggests that ions trapped at the F-SAM surface are strongly held and may be intertwined in the long alkyl chains. Resonance charge exchange between the incoming $Xe^{+\cdot}$ and the fluorocarbon chains leads to C–C bond cleavage that assists in release of the embedded ions. The energy dependence of the abundance ratio of m/z 145 and 173 is noticeably different from the previous case of ion m/z 134 and 91 (Fig. 4). One must suppose that the significant difference in size of m/z 134 and m/z 91, versus the smaller difference associated with the loss of CO between m/z 173 and 145, is responsible. The smaller structural change results in more similar steric hindrances and other binding forces, and thus the ions m/z 173 and 145 exhibit similar ejection efficiencies at all energies.

Similar experiments on the surface modified by deposition of the *m*-(trifluoromethyl)benzoyl cation were performed using NO^+ (m/z 30) as the sputtering projectile in the collision energy range of 25–70 eV. As expected, the smaller momentum transfer associated with NO^+ sputtering leads to less efficient release of the deposited ions—about 30% of the number of ion counts were produced compared to $Xe^{+\cdot}$ sputtering under the same conditions. Interestingly, the ion abundance ratio of m/z 145 and 173 again shows little dependence on the sputtering energy (Fig. 7), which is also in accord with the interpretation already offered.

4. Conclusion

Collisions of very low energy mass-selected polyatomic ions, such as the *N*,*N*-dimethyl-*p*-toluidine $(M\text{-}1)^+$ cation, allow their selective deposition onto a hydrocarbon self-assembled monolayer surface. This demonstrates the potential for soft landing of ions to be extended to a wide variety of surfaces, in addition to the fluorinated and cryogenic surfaces already reported on. The striking difference in the concomitant fragment ion abundance between the H-SAM and F-SAM surfaces indicated that the H-SAM surface is much “softer”—a phenomenon that is consistent with extensive results from energy transfer in the course of

surface-induced dissociation. The $(M-1)^+$ ion of the toluidine is largely intact after deposition at the H-SAM surface under conditions that result in extensive dissociation at the corresponding F-SAM surface. Dissociation of the soft-landing species occurs largely during the deposition process for both surfaces. Therefore, H-SAM surfaces are potentially beneficial for depositing less stable ions that might be dissociated readily at harder surfaces. The results show that using H-SAM surfaces as soft matrices opens the possibility for depositing labile ions.

The collision energy dependence for ejection of the deposited ions suggests that steric constraints play a crucial role in trapping the species at the surface. Smaller ions, sometimes only different by one or two substitutent groups, e.g. methyl groups, appear to bind more loosely at the interface and can be released at a relatively lower collision energy. In cases where this effect is avoided, an insignificant dependence of the fragment ion abundance on the collision energy of the sputtering projectile occurs and this points to the fact that dissociation occurs during the deposition rather than release stage. A large fraction of the energy imparted in the inelastic ion/surface collisions is believed to dissipate quickly into the "energy sink" represented by the surface. Little is converted into vibrational energy of the ejected ions.

It is found that soft-landed ions at F-SAM surfaces can be released at low collision energy. The appearance energy of the deposited substituted benzoyl ions approximately coincides with that of the chemical sputtering product CF_3^+ from the F-SAM surface ($\sim$ 18 eV $Xe^{+\cdot}$ sputtering energy). This supports the proposed mechanism that the deposited species may be intertwined with the long alkyl chains and high release efficiency is facilitated by C–C bond cleavage in the matrix. Nevertheless, there are several questions that remain to be answered, including (1) the chain length dependence of soft landing, and (2) the role of surface defects in the yield of soft landing. Studies on the effect of monolayer structure on the efficiency of ion trapping are currently underway. Preliminary data suggest that more highly organized surfaces (long assembly time, weeks) give higher trapping efficiencies.

Acknowledgement

This work was supported by the National Science Foundation (CHM-9732670). We thank Feng Wang for the gas-phase CID data.

References

[1] J. Shi, J.M. Kikkawa, R. Proksch, T. Schaffer, D.D. Awschalom, G. Medeiros-Ribeiro, P.M. Petroff, Nature 377 (1995) 707.
[2] (a) R.G. Wilson, R.G. Brewer, Ion Beams with Application to Ion Implantation, Wiley, New York, 1973; (b) J.F. Ziegler, Handbook of Ion Implantation Technology, North-Holland, New York, 1992; (c) G. Carter, W.A. Grant, Ion Implantation of Semiconductors, Wiley, New York, 1976.
[3] G. Scoles (Ed.), Atomic and Molecular Beam Methods, Oxford University Press, Oxford, 1988.
[4] A. Amirav, A. Danon, Int. J. Mass Spectrom. Ion Processes 97 (1990) 107.
[5] M.L. Hitchman, K.F. Jensen (Eds.), Chemical Vapor Deposition: Principles and Applications, Academic, San Diego, CA, 1993.
[6] J.W. Coburn, Pure Appl. Chem. 64 (1992) 709.
[7] J.-C. Lou, W.G. Oldham, H. Kawayoshi, P. Ling, J. Appl. Phys. 71 (1992) 3225.
[8] S.A. Miller, H. Luo, S. Pachuta, R.G. Cooks, Science 275 (1997) 1447.
[9] H. Luo, S.A. Miller, R.G. Cooks, Int. J. Mass Spectrom. Ion Processes 174 (1998) 193.
[10] J.T. Godbout, T.M. Halasinski, G.E. Leroi, J. Allison, J. Phys. Chem. 100 (1996) 2892.
[11] A.P. Alivisatos, Science 271 (1996) 933.
[12] See R.P. Andres, J.D. Bielefeld, J.I. Henderson, D.B. Janes, V.R. Kolagunta, C.P. Kubiak, W.J. Mahoney, R.G. Osifchin, 273 (1996) 1690, and references therein.
[13] R.G. Cooks, T. Ast, M.A. Mubud, Int. J. Mass Spectrom. Ion Processes 100 (1990) 209.
[14] A.R. Dongre, A. Somogyi, V.H. Wysocki, J. Mass Spectrom. 31 (1996) 339.
[15] W.Q. Zhong, E.N. Nikolaev, J.H. Futrell, V.H. Wysocki, Anal. Chem. 69 (1997) 2496.
[16] W.R. Koppers, J.H.M. Beijersbergen, K. Tsumori, T.L. Weeding, P.G. Kistemaker, A.W. Kleyn, Surf. Sci. 357 (1996) 678.
[17] T. Pradeep, D.E. Riederer Jr., S.H. Hoke II, T. Ast, R.G. Cooks, M.R. Linford, J. Am. Chem. Soc. 116 (1994) 8658.
[18] R.G. Cooks, T. Ast, T. Pradeep, V. Wysocki, Acc. Chem. Res. 27 (1994) 316.
[19] M.J. Hayward, F.D.S. Park, L.M. Phelan, S.L. Bernasek, A. Somogyi, V.H. Wysocki, J. Am. Chem. Soc. 118 (1996) 8375.
[20] T.G. Schaaff, Y. Qu, N. Farrell, V.H. Wysocki, J. Mass Spectrom. 33 (1998) 436.
[21] S. Hayakawa, B. Feng, R.G. Cooks, Int. J. Mass Spectrom. 167 (1997) 525.

[22] H. Lim, D.G. Schultz, E.A. Gislason, L. Hanley, J. Phys. Chem. B 102 (1998) 4573.
[23] C. Gu, V.H. Wysocki, J. Am. Chem. Soc. 119 (1997) 12010.
[24] B. Feng, J. Shen, V. Grill, C. Evans, R.G. Cooks, J. Am. Chem. Soc. 120 (1998) 89.
[25] S.B. Wainhaus, H.J. Lim, D.G. Schultz, L. Hanley, J. Chem. Phys. 106 (1997) 10329.
[26] M.C. Yang, C.H. Hwang, H. Kang, J. Chem. Phys. 107 (1997) 2611.
[27] A.A. Tsekouras, M.J. Iedema, G.B. Ellison, J.P. Cowin, Int. J. Mass Spectrom. Ion Processes 174 (1998) 219.
[28] Personal communication.
[29] M.R. Morris, D.E. Riederer, B.E. Winger, R.G. Cooks, T. Ast, C.E. Chidsey, Int. J. Mass Spectrom. Ion Processes 122 (1992) 181.
[30] K. Vékey, A. Somogyi, V.H. Wysocki, J. Mass Spectrom. 30 (1995) 212.
[31] J.H. Callahan, A. Somogyi, V.H. Wysocki, Rapid Commun. Mass Spectrom. 7 (1993) 693.
[32] B.E. Winger, H.J. Laue, S.R. Horning, R.K. Julian Jr., S.A. Lammert, D.E. Riederer Jr., R.G. Cooks, Rev. Sci. Instrum. 63 (1992) 5613.
[33] R.G. Cooks, A.L. Rockwood, Rapid Comm. Mass Spectrom. 5 (1991) 93.
[34] J.C. Schwartz, A.P. Wade, C.G. Enke, R.G. Cooks, Anal. Chem. 101 (1990) 1.
[35] C.E.D. Chidsey, C.R. Bertozzi, T.M. Putvinski, A.M. Mujsce, J. Am. Chem. Soc. 112 (1990) 4301.
[36] M. Vincenti, R.G. Cooks, Org. Mass Spectrom. 23 (1988) 317.
[37] S.G. Lias, J.E. Bartmess, J.F. Liebman, J.H. Holmes, R.D. Levin, W.G. Mallard, J. Phys. Chem. Ref. Data 17 (1988) (Suppl.).
[38] W.G. Mallard (Ed.), NIST World Wide Web Standard Reference Database, 1997, http://webbook.nist.gov
[39] S.A. Miller, D.E. Riederer Jr., R.G. Cooks, W.R. Cho, H.W. Lee, H. Kang, J. Phys. Chem. 98 (1994) 245.